COMMUNICATION TO THE EDITOR

BIOTECHNOLOGY and BIOENGINEERING

Microprinted Feeder Cells Guide Embryonic Stem Cell Fate

Hossein Tavana,[1,2] Bobak Mosadegh,[2] Parsa Zamankhan,[2] James B. Grotberg,[2] Shuichi Takayama[2,3,4]

[1]Department of Biomedical Engineering, University of Akron, Akron, Ohio

[2]Department of Biomedical Engineering, University of Michigan, Ann Arbor, Michigan 48109; telephone: +1-734-615-5539; fax: (734) 936-1905; e-mail: takayama@umich.edu

[3]Department of Macromolecular Science and Engineering, University of Michigan, Ann Arbor, Michigan

[4]Division of Nano-Bio and Chemical Engineering WCU Project, UNIST, Ulsan, Republic of Korea

Received 18 January 2011; revision received 26 March 2011; accepted 15 April 2011

Published online 2 May 2011 in Wiley Online Library (wileyonlinelibrary.com). DOI 10.1002/bit.23190

ABSTRACT: We introduce a non-contact approach to microprint multiple types of feeder cells in a microarray format using immiscible aqueous solutions of two biopolymers. Droplets of cell suspension in the denser aqueous phase are printed on a substrate residing within a bath of the immersion aqueous phase. Due to their affinity to the denser phase, cells remain localized within the drops and adhere to regions of the substrate underneath the drops. We show the utility of this technology for creating duplex heterocellular stem cell niches by printing two different support cell types on a gel surface and overlaying them with mouse embryonic stem cells (mESCs). As desired, the type of printed support cell spatially direct the fate of overlaid mESCs. Interestingly, we found that interspaced mESCs colonies on differentiation-inducing feeder cells show enhanced neuronal differentiation and give rise to dense networks of neurons. This cell printing technology provides unprecedented capabilities to efficiently identify the role of various feeder cells in guiding the fate of stem cells.

Biotechnol. Bioeng. 2011;108: 2509–2516.

KEYWORDS: polymeric aqueous two-phase system; cell printing; cell microenvironment engineering; cell–cell contact; embryonic stem cell fate

Direct homotypic and heterotypic intercellular interactions have major regulatory effects on self-renewal and differentiation of stem cells during normal development (Chen et al., 2007; Tsai and McKay, 2000). Advances in cell patterning techniques have made it possible to create simple, yet well-controlled, in vitro niches and systematically study the role of cell–cell contact on various cellular phenotypes. The majority of patterning approaches are often indirect. Microfabricated elastomeric stamps transferring cell adhesion molecules onto a substrate (Chen et al., 1997), elastomeric masks containing through-holes (Cho et al., 2008), and photoresponsive surfaces (Kikuchi et al., 2009) allow planar patterning of mostly two cell types.

Direct patterning of cells on gel substrates has been realized using the contact of cell-loaded solid pins with the substrate (Fernandes et al., 2010). The use of microfabricated microwells enables direct positioning of cells onto an existing cell layer, though with limited spatial control (Rosenthal et al., 2007) and efficiency (Khademhosseini et al., 2006). Thermoresponsive polymers accommodate stacking of layers of cells but only as cell sheets (Yang et al., 2009). Customized thermal and piezoelectric inkjet printers allow direct printing of cells (Cui et al., 2010) although there are concerns over cell membrane damage, reduced cellular viability, and pattern fidelity. Extrusion of gel-encapsulated cells onto substrates by mechanical means also results in layering of cells but with impaired direct cell–cell contact due to gel encapsulation (Moon et al., 2010).

We have described a new technique for direct non-contact printing of biomaterials onto a cell monolayer. The method utilizes a polymeric aqueous two-phase system (ATPS) consisting of polyethylene glycol (PEG) and dextran (DEX)

Correspondence to: S. Takayama

Contract grant sponsor: NIH
Contract grant number: HL084370
Contract grant sponsor: LSI-CCG Thermo Fisher Scientific Collaborative Pilot Project
Additional Supporting Information may be found in the online version of this article.

as the phase forming polymers (Albertsson, 1986) and allows autonomous dispensing of nanoliters of the DEX phase containing biomaterials of interest onto a monolayer of cells maintained in the immersion PEG phase. We have shown the feasibility of this approach for direct and localized printing of small molecules (Tavana et al., 2009), specifically liposomal and lentiviral transfection reagents, as well as living cells (Tavana et al., 2010) onto a monolayer of cells. This method accommodated a layered co-culture system when the printed cell type was different from the cell monolayer. Gentle and contact-free printing of cells helps retain full viability and functionality of both printing and surface layer cells. Using this technique, we created standalone printed mouse embryonic stem cell (mESC) colonies on a monolayer support PA6 stromal cells and showed that neuronal differentiation of individual colonies significantly enhances with the colony size (Tavana et al., 2010). Here, we broaden the utility of this microtechnology for simultaneous screening of the role of different feeders and interrogate the fate of overlaid mESCs. The present study offers novel technological and biological findings different from our previous work. Technologically, it enables (i) generating defined size clusters of different feeders over a hydrogel substrate with pre-defined interspacing and (ii) creating distinct stem cell niches comprised of different feeder clusters in the same culture plate. Biologically, it (i) allows selective feeder type-guided fate determination of stem cells, (ii) demonstrates that interspacing between mESC colonies residing on stromal PA6 feeder clusters is an important determinant of neuronal differentiation efficiency of mESCs, and (iii) feeder-mediated cues are short range and sufficiently local to allow differentiation or maintenance of pluripotency of mESCs on neighboring clusters of different feeders.

To generate a duplex cell microarray, the two cell types are each separately mixed with the DEX phase and the resulting suspensions are transferred into a 1,536-well plate. Slot pins mounted on a fixture are dipped into the wells to load with the cell-containing DEX phase. Pins are slowly withdrawn from the source plate and dipped into a culture plate containing the PEG phase (Fig. 1a). Due to an extremely low interfacial tension and density difference between the two phases, the denser DEX phase dispenses and forms distinct droplets of cell suspension on the plate (Fig. 1b). The culture plate is incubated for 3 h to allow cells to adhere to the substrate. The fully aqueous two-phase cell culture media nourish cells during this incubation time and eliminate the need for further media addition that would disturb the printed patterns. After cells attach, the ATPS is washed out and replaced with regular culture media (Fig. 1c). This process results in uniform size islands of two different cell types with defined interspacing. Figure 2a–c shows a printed a microarray of green and red fluorescently labeled mouse myoblast C2C12 cells in a checkerboard pattern without any cross contamination between cell clusters during the printing process (Fig. 2a). It is noted the size of cellular islands can increase over time and eventually, the initially

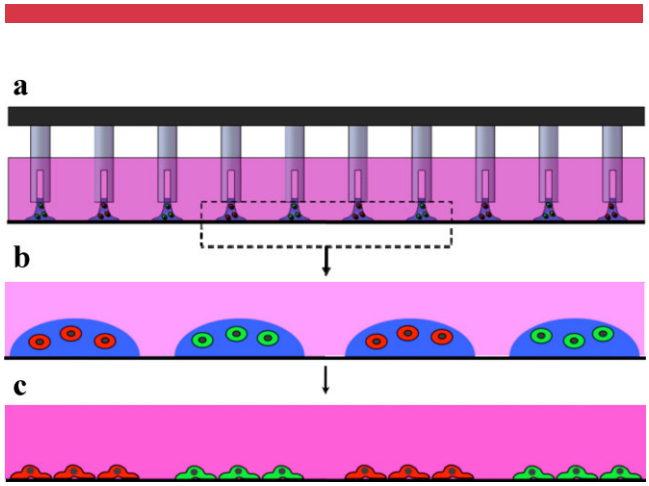

Figure 1. Aqueous two-phase duplex cell printing. **a**: Nanoliter volume pins dispense DEX phase-cell suspension onto the surface immersed in the PEG phase. **b**: Distinct droplets with defined interspacing and containing different cells form on the culture plate. **c**: Incubation results in adhered clusters of two different cell types. [Color figure can be seen in the online version of this article, available at http://wileyonlinelibrary.com/bit]

interspaced cell clusters will meet. The time for this process depends on the initial size of clusters, their interspacing, and cellular growth rate. With the configuration of Figure 2a, that is, ~800 μm diameter of cellular islands and 2.25 mm interspacing, the peripheries of C2C12 clusters meet in about 4–5 days of culture.

In principle, this technique accommodates printing many different cell types on the same substrate in a single step without using immobilized cell adhesion molecules required with microfabrication-mediated cell patterning approaches. Each cell cluster of the microarray was printed using a 200 nL pin, which generated a ~800 diameter cell spots. For a printing density of 2.5×10^6/mL C2C12 cells, each spot contained 255 ± 41 cells. The seeding density, and hence the number of cells per spot, can be adjusted for different cell types depending on the size of cells after they spread. Changing the dispensing pin volume varies the size of the printed cell clusters. Spots as small as 240 μm can be printed using a 20 nL pin (Fig. 2d).

We utilized this capability to microprint different support cell types over a hydrogel substrate to study the fate of mESCs in heterocellular microenvironments. 1.2 mm spots of PA6 stromal cells and mouse embryonic fibroblasts (MEF) were printed on a porcine gel-coated culture plate with a center-to-center spacing of 4.5 mm (Fig. 3a, left panel), which is equivalent to well-to-well spacing of a 384 microwell plate. After feeder cells spread and formed tight clusters in about 24 h, they were overlaid with mESCs randomly seeded everywhere in the culture plate (Fig. 3a, right panel). The culture system was maintained for 8 days and mESCs proliferated on feeder clusters as well as in spaces outside feeder clusters. Next, mESCs everywhere in the culture plate were examined for the neuron-specific class III β tubulin TuJ1 differentiation marker. The MEF feeder layer supported prolonged undifferentiated state of mESCs

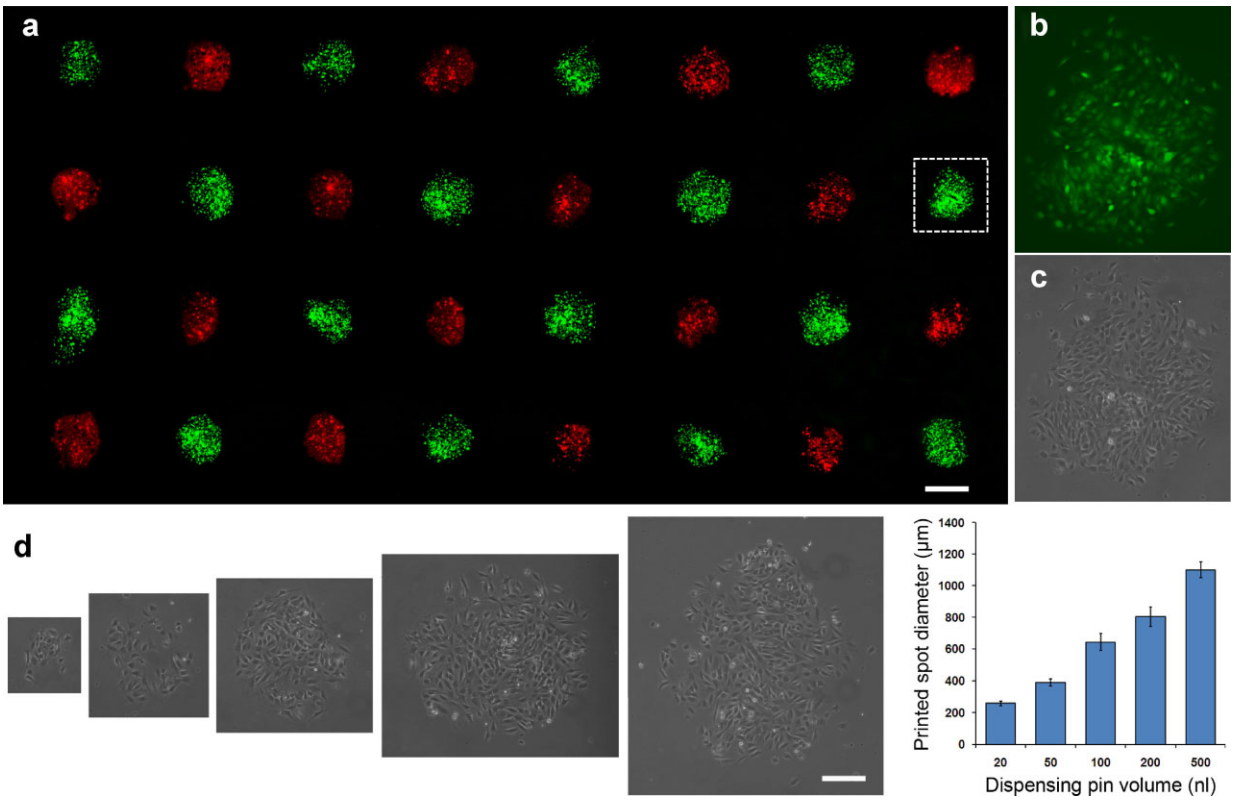

Figure 2. Duplex printed cell microarray. **a**: An 8 × 4 printed microarray of C2C12 cells stained with green cell and red cell tracking stains. **b,c**: Magnified fluorescent and brightfield images of the boxed spot. **d**: The size of printed spot of cells varies proportional to the volume of dispensing cell suspension in DEX phase within the range 20–500 nL. Scale bar 800 μm in (a). [Color figure can be seen in the online version of this article, available at http://wileyonlinelibrary.com/bit]

without significant expression of the neuronal marker TuJ1 (Fig. 3b and c and Supporting Information Fig. SI-1). On the other hand, screening mESC-PA6 co-culture islands showed that mESC colonies stained positive and showed significant neuronal differentiation on PA6 feeder clusters (Fig. 3b and d). Great majority of cells proliferating outside feeder clusters did not show neuronal differentiation marker although we observed few scattered differentiated cells too (noted in Fig. 3b schematics). This population was not characterized.

Major differences in the morphology of mESCs were also observed on the two types of printed feeder cells. On the MEF cell clusters, mESCs grew and remained as tight colonies for the entire culture period (Fig. 3e and Supporting Information Fig. SI-2a) whereas significant migration of mESCs to the colony periphery and into the space among the colonies occurred on PA6 spots (Fig. 3f and Supporting Information Fig. SI-2b). This observation is in agreement with previous findings that differentiating cells first migrate to the periphery of the colonies (Vazin et al., 2008) and may take place to generate space for extension of neuronal processes. Close scrutiny of the differentiated colonies on PA6 feeder cells showed that extensive processes stretched between adjacent mESC colonies and a large number of thick neurite bundles formed (Fig. 3g and h).

Importantly, mESC colonies on MEF support cell clusters in the same culture system with PA6 cells islands remained undifferentiated suggesting that direct mESC-feeder heterocellular contact and short range diffusive soluble factors play a dominant role in dictating the mESC fate. Any lineage commitment inducing factors that support neuronal differentiation of mESC colonies on PA6 spots do not perturb the undifferentiated state of mESCs on MEF clusters. Such conclusions about effects of direct heterocellular interactions and soluble cues on the fate of stem cells would be difficult to reach with separate co-cultures of mESCs with the two support cell types in a microwell plate configuration.

In Figure 3d, multiple small mESC colonies of ~100–300 μm in diameter are located within close proximity of one another with spacings of ~50–150 μm. The total mESC colony area is 0.15 mm^2. We quantified the total fluorescent intensity of TuJ1 expression of this and similar configurations of mESC colonies ($n = 6$) differentiated on PA6 feeder spots as a measure of differentiation efficiency and obtained an average net staining of 8.36 ± 2.03 a.u. for an average multi-colony configuration area of the $0.15 \pm 0.03\ mm^2$

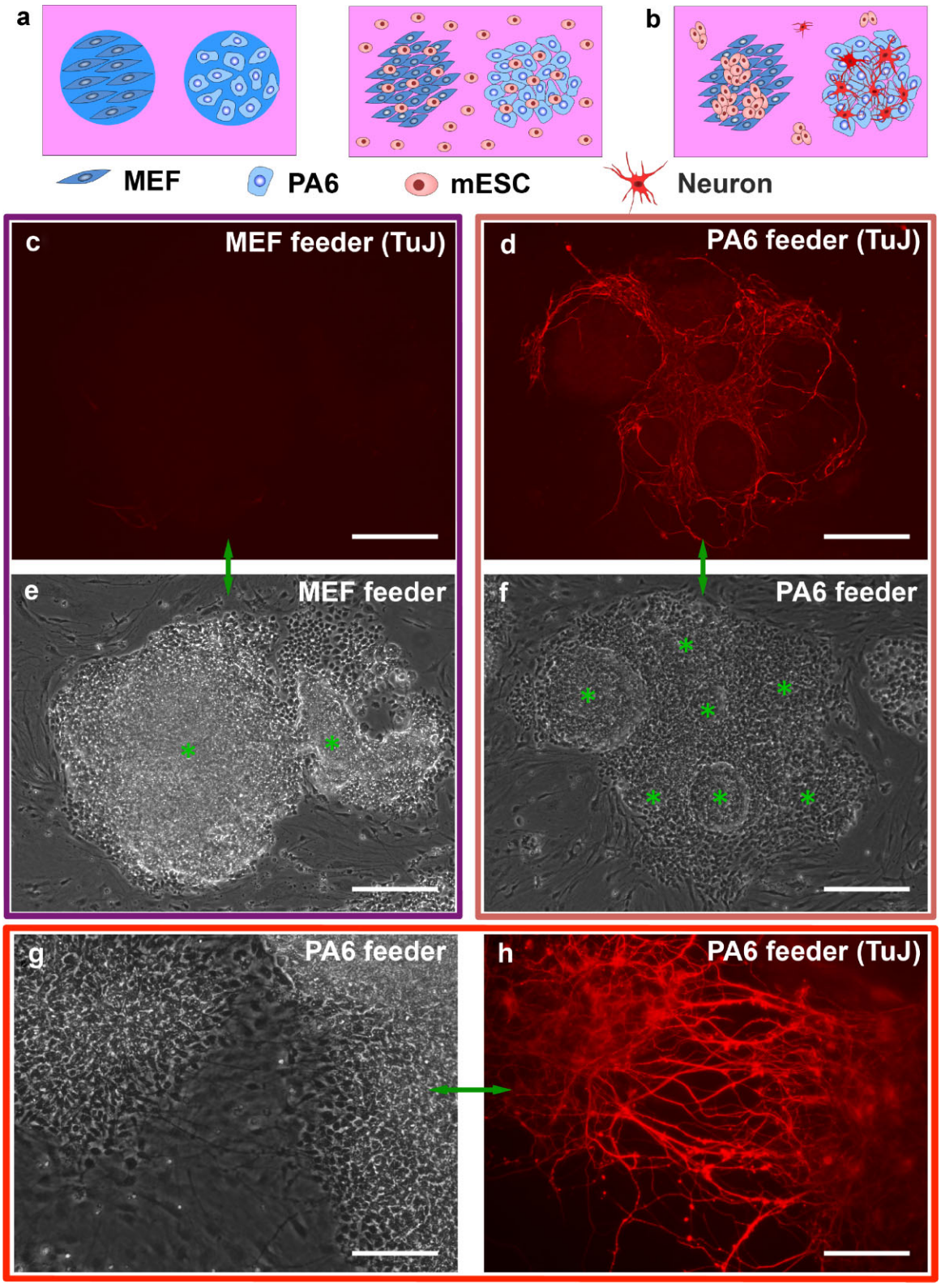

Figure 3. Engineering duplex mESC microenvironments. **a**: Schematics of printing PA6 and MEF feeder spots using the ATPS approach and subsequently overlaying the spots of cells with mESCs at day 0. **b**: Schematics of neuronal differentiation of mESCs on feeder PA6 spot but not on the MEF spot. **c**: Representative image of lack of TuJ staining of mESC on a MEF feeder spot. **d**: Representative image of neuronal-specific TuJ1 expressing colonies on a PA6 feeder spot. **e**,**f**: Brightfield images of mESC colonies on MEF and PA6 spots. mESC colonies are noted with asterisks. Comparison with corresponding TuJ staining images (c,d) helps identify the location of colonies and migrated cells. **g**,**h**: Brightfield and TuJ1 neuronal marker staining of mESC colonies on a PA6 feeder spot at high magnification, The colonies show extensive bundles of intercolony processes. Scale bar 250 μm in (c–f) and 100 μm in (g,h). The images correspond to day 8 of co-culture. The schematics are not to scale. [Color figure can be seen in the online version of this article, available at http://wileyonlinelibrary.com/bit]

($n = 6$). We have previously demonstrated that individual mESC colonies maintained on a PA6 support monolayer show enhanced differentiation efficiency, as measured by TuJ1 expression, with increase in the colony size. Interestingly, the net TuJ1 expression in Figure 3d is almost on the scale of the net fluorescent signal intensity of 10.02 ± 2.17 a.u. resulted from individual mESC colonies of $5.83 \pm 0.49\,mm^2$ on the PA6 feeder ($n = 5$) (Tavana et al., 2010). Normalizing the data with respect to total colony area indicates that patterned multiple colonies of Figure 3d yield one order of magnitude increase in the differentiation efficiency. We confirmed the significance of this finding by carrying out a statistical *t*-test that resulted in a value of $P < 0.01$. This result suggests that, in addition to the mESC colony size effect demonstrated previously, colony interspacing is a major regulator of mESC differentiation to neurons. While support cells provide necessary differentiation-promoting cues such as cell surface-bound factors or secreted factors secondarily tethered to PA6 cell surface (Kawasaki et al., 2000), signaling between adjacent mESC colonies significantly enhances the quality of neuronal differentiation. The intercolony signaling is most likely mediated synergistically by several neurite outgrowth promoting factors including endogenous (autocrine) soluble factors (Calabrese, 2008) produced in adjoining ES colonies, exogenous (paracrine) soluble factors secreted by feeder cells (Kawasaki et al., 2000), and non-neuronal differentiated cells (Roth et al., 2007) within those aggregates.

We evaluated the role of autocrine signaling in differentiation of small, closely positioned mESC colonies of Figure 3d by a finite element modeling of diffusion of endogenous soluble factors in the culture using the following two-dimensional diffusion equation:

$$\frac{\partial c}{\partial t} = D\nabla^2 c \qquad (1)$$

Our initial modeling showed the steady-state condition is attained within only 1 h. Since the duration of co-culture is substantially longer (8 days), we performed the simulation under a steady-state condition and modeled the concentration profile across the bottom surface where the colonies are located. In Equation (1), c is the concentration of soluble factors and $D \approx 1 \times 10^{-6}\,cm^2\,s^{-1}$ is the diffusion coefficient (Hui and Bhatia, 2007). Each mESC colony was approximated as a circular area. The size and interspacing of colonies were set using configuration in Figure 3d. To set the boundary condition, we determined the distance from the cluster of colonies where the concentration of autocrine factors becomes negligible ($\sim 10^{-7}$ times the maximum concentration). This resulted in a distance of 0.5 cm in each direction and thus, a $1 \times 1\,cm^2$ simulation domain.

We compared the distribution of secreted factors from this multicolony configuration with that of an individual standalone mESC colony whose area would be equal to the cumulative area of colonies in Figure 3d. The modeling result and 2D plots of concentration of autocrine factors are shown in Figure 4. In case of the individual colony, the concentration is highest at the center of the colony, drops toward its periphery, and quickly diminishes away from the periphery (Fig. 4a and b). This type of autocrine factor gradient may restrict neurons and their processes to the immediate periphery of the mESC colony, significantly limiting neurite development and extension (Fig. 4c). On the other hand, multiple small colonies exhibit a lower maximum concentration but an asymmetric concentration profile that consists of several local increases in the gradient of concentration in the spacing among the colonies (Fig. 4d and e). Overlaying the concentration profile and TuJ staining images shows abundance of neuronal extensions where stable concentration gradients exist (Fig. 4f). We postulate that maintenance of concentration gradients in the case of multi-colony configuration provides guiding cues for the migration and neuronal differentiation of mESCs. Differentiated cells extend neurites mainly toward the inner periphery of the colonies, where colonies face each other, enhancing the development of neuronal processes that stain for TuJ1. Close scrutiny of Fig. 3d and similar differentiated colonies (Supporting Information Fig. SI-3a and c) supports this view. TuJ1 expression levels are highest in areas between mESC colonies and significantly reduce at their outer periphery where the concentration of soluble factors decreases sharply. Analysis of the TuJ expression intensity along the line scan of Figure 4c and f shows that localized TuJ expression correlates well with the corresponding concentration gradient profile (Fig. 4g and h). Maintenance of concentration gradient of soluble factors among interspaced colonies also helps regulate the dense network of neuronal processes (Rosoff et al., 2004). Although the actual concentrations of autocrine factors are not known, this model provides a qualitative explanation that short-range concentration gradients of endogenous soluble factors in part give rise to differentiation patterns similar to that in Fig. 3d and Supporting Information Fig. SI-3. We emphasize that in addition to autocrine factors concentration gradient, several other mechanisms synergistically regulate the neuronal differentiation of mESC colonies on stromal support cells.

This aqueous biphasic cell printing technology allows direct and contact-free positioning of multiple cell types onto delicate substrates in a single step. Duplex co-culture of mESCs with MEF and PA6 feeder cells on a hydrogel surface enabled, for the first time, to confirm that the effect of support cell layer is sufficient yet local such that overlaid mESCs either remain undifferentiated or undergo neuronal differentiation according to the underlying support cell type. Interestingly, on differentiation-promoting PA6 cell clusters, mESC colonies interspaced in close proximity of one another show very efficient neuronal differentiation patterns compared to standalone mESC colonies, due in part to concentration gradients of autocrine factors. Overall, this microtechnology is useful to create multiplexed ES cell

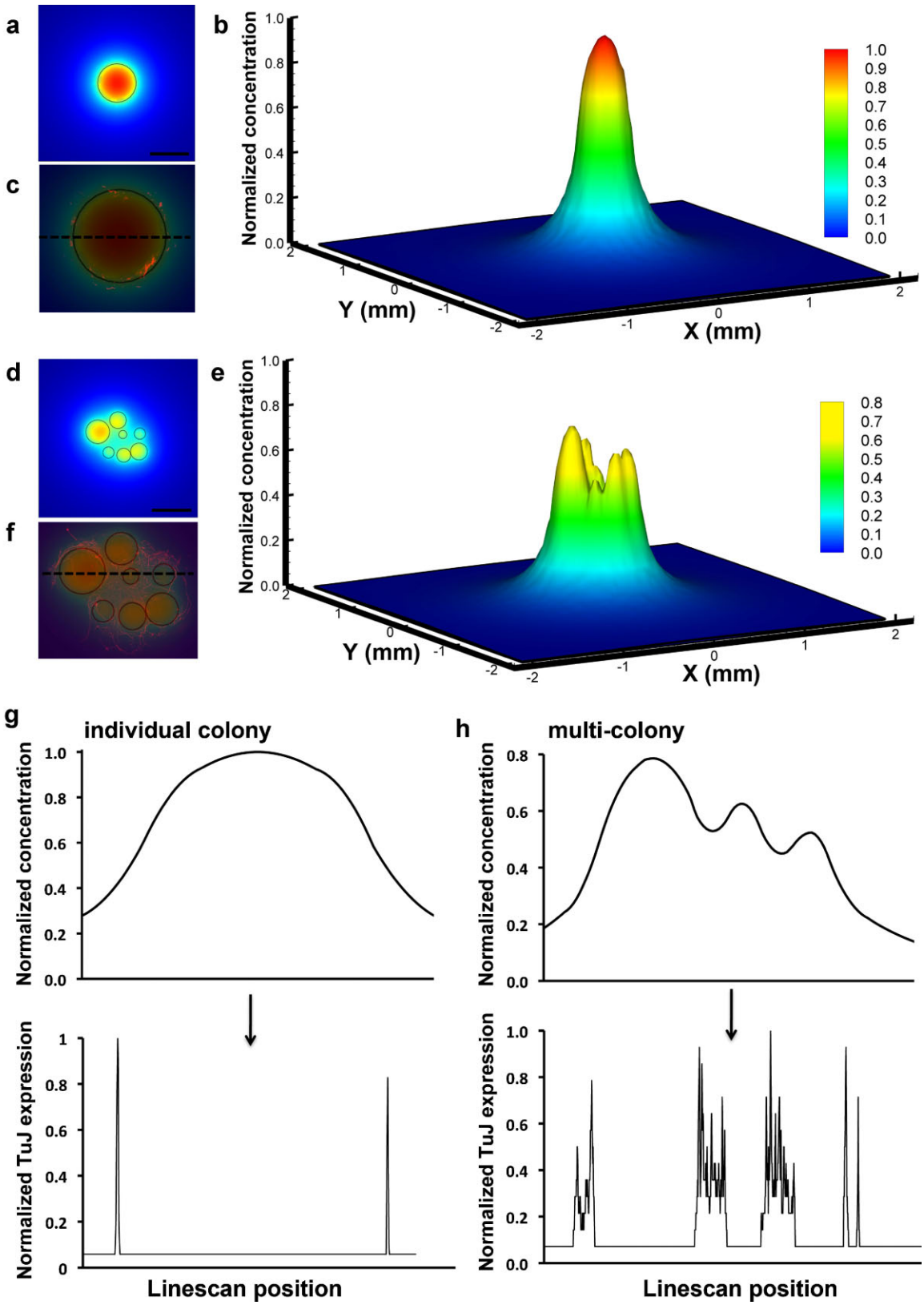

Figure 4. Finite element modeling of mESC-secreted autocrine factors. Concentration profiles of diffusive autocrine signaling factors for (**a**,**b**) an individual colony of similar area to the multi-colony configuration of Fig. 3d, (**c**) overlay of magnified concentration map and TuJ expression of the individual colony shows that the minimal TuJ expression is limited to the periphery of the colony, (**d**,**e**) modeling result of the multiple interspaced colonies of Fig. 3d shows a significantly different distribution of factors from that of the individual colony, (**f**) overlay of magnified concentration map and TuJ expression of the multi-colony configuration shows significant TuJ expression in spacing among colonies, (**g**,**h**) typical line scans of concentration profile for the individual and the multi-colony configurations along the dashed lines of panel c and f show that fluorescent intensity of TuJ expression correlates well with local concentration gradients. Scale bar 500 μm in (a) and (d). [Color figure can be seen in the online version of this article, available at http://wileyonlinelibrary.com/bit]

microenvironments and identify the role of different support cells in guiding the fate decisions of ES cells in a cell and reagent efficient manner. This approach will also benefit various studies where direct heterocellular contact is a major regulator of cellular functions.

Experimental Methods

Preparation of Two-Phase Media, PA6 and MEF Feeder Cell Spots, and Culture of mESCs

PEG (2.5% (w/w); M_w: 35K, Fluka, St. Louis. MO) and 6.4%(w/w) DEX (M_w: 500K, Pharmacosmos, Holbaek, Denmark) solutions were prepared in culture media. Skull bone marrow derived PA6 cells (Riken, Tokyo, Japan) were provided by K. Hiroaki and grown in α-MEM (Invitrogen, Grand Island, NY) supplemented with 10% heat-inactivated fetal bovine serum (FBS, Invitrogen) and 1% antibiotic (Invitrogen). Cells were grown to a desired confluence and mitotically inactived by 10 μg/mL mitomycin C (Sigma, St. Louis, MO) treatment for 2 h. MEF cells, which were also rendered mitotically inactive by cesium irradiation, were received from the University of Michigan Transgenic Core. Cell suspensions were each thoroughly mixed with an equal volume of the DEX phase to a 3.2% concentration. Spots of PA6 and MEF cells were printed from final cell suspension densities of 7.0×10^5 and 1.5×10^6/mL, respectively, on porcine gel-coated 6-well plates using 500 nL volume dispensing pins. Cells were grown for 24–48 h in above media to spread. Then, a conditioning media consisting of G-MEM (Invitrogen), 10% knockout serum replacement (KSR, Invitrogen), 0.1 mM non-essential amino acids (Invitrogen), 2 mM glutamax (Invitrogen), 1 mM sodium pyruvate (Sigma), and 0.1 mM 2-mercaptoethanol (Sigma) was used to incubate feeder cells at 37°C, 5% CO_2, and 95% humidity overnight before seeding mESCs.

mESCs were provided by S. O'Shea. Cells were cultured in 1 mg/mL porcine gel-coated Petri dishes using G-MEM with 10% KSR, 1% FBS, 0.1 mM non-essential amino acids, 1 mM sodium pyruvate, 0.1 mM 2-mercaptoethanol, and 2×10^3 U/mL leukemia inhibitory factor (LIF, Millipore, Billerica, MA). mESCs were seeded at a density of 8,000 cells per each well of a 6-well plate containing the printed spots of PA6 and MEF (day 0). mESCs were cultured for eight more days to form colonies from single cells. Culture media was changed on day 4 and then every other day.

Immunofluorescence, Imaging, and Image Analysis

At day 8 of culture, mESC colonies were fixed in −20°C methanol for 6 min, washed three times with PBS and twice with PBS containing 5% BSA as the blocking reagent. The primary antibody rabbit neuronal class III-β-tubulin (TuJ1) mAb (Covance, Princeton, NJ) was diluted in PBS/5% BSA at a concentration of 1 μg/mL and added to fixed cells for 1 h at room temperature. After washing, the primary antibody was visualized with fluorescently labeled goat anti-rabbit IgG (Jackson ImmunoResearch, West Grove, PA) at a concentration of 3 μg/mL and incubated for 1 h. Then cells were washed three times with PBS. We imaged cells using an inverted fluorescence microscope (Nikon, Melville, NY, TE300). We used SimplePCI (Compix, Irvine, CA) to measure fluorescence intensity and the area of differentiated mESC colonies.

We acknowledge the financial support from an NIH grant (HL084370), LSI-CCG Thermo Fisher Scientific Collaborative Pilot Project, and a gift from J. Passino.

References

Albertsson P-A. 1986. Partition of cell particles and macromolecules. New York: John Wiley & Sons, Inc.

Calabrese EJ. 2008. Enhancing and regulating neurite outgrowth. Crit Rev Toxicol 38:391–418.

Chen CS, Mrksich M, Huang S, Whitesides GM, Ingber DE. 1997. Geometric control of cell life and death. Science 276:1425–1428.

Chen SS, Fitzgerald W, Zimmerberg J, Kleinman HK, Margolis L. 2007. Cell–cell and cell–extracellular matrix interactions regulate embryonic stem cell differentiation. Stem Cells 25:553–561.

Cho CH, Berthiaume F, Tilles AW, Yarmush ML. 2008. A new technique for primary hepatocyte expansion in vitro. Biotechnol Bioeng 101:345–356.

Cui X, Dean D, Ruggeri ZM, Boland T. 2010. Cell damage evaluation of thermal inkjet printed Chinese hamster ovary cells. Biotechnol Bioeng 106:963–969.

Fernandes TG, Kwon S-J, Bale SS, Lee M-Y, Diogo MM, Clark DS, Cabral JMS, Dordick JS. 2010. Three-dimensional cell culture microarray for high-throughput studies of stem cell fate. Biotechnol Bioeng 106:106–118.

Hui EE, Bhatia S. 2007. Micromechanical control of cell–cell interactions. Proc Natl Acad Sci 104:5722–5726.

Kawasaki H, Mizuseki K, Nishikawa S, Kaneko S, Kuwana Y, Nakanishi S, Nishikawa S, Sasai Y. 2000. Induction of midbrain dopaminergic neurons from ES cells by stromal cell-derived inducing activity. Neuron 28:31–40.

Khademhosseini A, Ferreira L, Yeh J, Blumling J, Fukuda J, Eng G, Langer R. 2006. Co-culture of human embryonic stem cells with murine embryonic fibroblasts on microwell-patterned substrates. Biomaterials 27: 5968–5977.

Kikuchi K, Sumaru K, Edahiro J-I, Ooshima Y, Sugiura S, Takagi T, Kanamori T. 2009. Stepwise assembly of micropatterned co-cultures using photoresponsive culture surfaces and its application to hepatic tissue arrays. Biotechnol Bioeng 103:552–561.

Moon S, Hasan SK, Song YS, Xu F, Keles HO, Manzur F, Mikkilineni S, Hong JW, Nagatomi J, Haeggstrom E, et al. 2010. Layer by layer three-dimensional tissue epitaxy by cell-laden hydrogel droplets. Tissue Eng C 16:157–166.

Rosenthal A, Macdonald A, Voldman J. 2007. Cell patterning chip for controlling the stem cell microenvironment. Biomaterrials 28:3208–3216.

Rosoff WJ, Urbach JS, Esrick MA, McAllister RG, Richards LJ, Goodhill GJ. 2004. A new chemotaxis assay shows the extreme sensitivity of axons to molecular gradients. Nat Neurosci 7:678–682.

Roth TM, Ramamurthy P, Ebisu F, Lisak RP, Bealmear BM, Barald KF. 2007. A mouse embryonic stem cell model of Schwann cell differentiation for studies of the role of neurofibromatosis type 1 in Schwann cell development and tumor formation. Glia 15:1123–1133.

Tavana H, Jovic A, Mosadegh B, Lee QY, Liu X, Luker KE, Luker GD, Weiss SJ, Takayama S. 2009. Nanoliter liquid patterning in aqueous environments for spatially-defined reagent delivery to mammalian cells. Nat Mater 8:736–741.

Tavana H, Mosadegh B, Takayama S. 2010. Polymeric aqueous biphasic systems for non-contact cell printing on cells: Engineering heterocellular embryonic stem cell niches. Adv Mater 22:2628–2631.

Tsai RYL, McKay RDG. 2000. Cell contact regulates fate choice by cortical stem cells. J Neurosci 20:3725–3735.

Vazin T, Chen J, Lee C-T, Amable R, Freed WJ. 2008. Assessment of stromal-derived inducing activity in the generation of dopaminergic neurons from human embryonic stem cells. Stem Cells 26:1517–1525.

Yang J, Yamato M, Sekine H, Sekiya S, Tsuda Y, Ohashi K, Shimizu T, Okano T. 2009. Tissue engineering using laminar cellular assemblies. Adv Mater 21:3404–3409.